SHEAR LAYER INSTABILITIES IN AN IMPULSIVELY STARTED AIRFOIL

Anushka Goyal
Department of Mechanical Engineering
McGill University
817 Sherbrooke Street West, Montréal, Québec H3A 0C3, Canada
anushka.goyal@mail.mcgill.ca

Jovan Nedić
Department of Mechanical Engineering
McGill University
817 Sherbrooke Street West, Montréal, Québec H3A 0C3, Canada
jovan.nedic@mcgill.ca

ABSTRACT

We investigate the onset of shear layer instabilities in the wake of an impulsively started NACA0010 airfoil at low angles of attack and various surge speeds and distances. The wake consists of a primary starting vortex, shear layers shed by the leading and trailing edges. Two distinct flow regimes are defined at a given angle of attack: one where the shear layer remains intact at speeds lower than a critical surge speed (U_{critical}) and another at speeds greater than U_{critical} where the shear layer breaks into secondary Kelvin-Helmholtz type vortices. The shear layer is discretised into patches of vorticity and the velocity field in each vortex patch is studied and salient differences between the two cases are investigated.

INTRODUCTION

It is well established that an airfoil impulsively set into linear motion will result in the formation of a starting vortex, as well as a shear layer with the same sense of vorticity. For steady flows, the wake of an airfoil has been characterised and different wake modes have been identified, depending on the angle of attack and Reynolds number (Huang & Lin, 1995). For unsteady or impulsively started flows, there is a plethora of studies that discuss the wake (Fernando & Rival, 2016) as well as the leading edge vortex (Ford & Babinsky, 2013) at high, post stall angles of attack. There are also studies that look at impulsively rotated plates (DeVoria & Ringuette, 2012; Francescangeli & Mulleners, 2023). However, the characteristics of the unsteady wake of an impulsively started airfoil at low angles of attack has not been studied to the best of the authors' knowledge. The objective of the present study is to characterise shear layers shed by impulsively started airfoils at low angles of attack at various surge speeds. Of particular interest is understanding the necessary conditions for instabilities to develop in the shear layer.

EXPERIMENTAL SETUP

The experiment is designed for a 30 inch long, 12.5 inch wide and 19 inch deep water tank. The vortex generating airfoil with a NACA0010 profile is machined in aluminium and anodised, with a span of 17.5 inches and chord size of 2.9 inches. It is further attached with end plates to ensure that 2D line vortices are generated. The airfoil is towed through various surge distances along the width of the tank using a Newmark LC Series 300 mm linear traverse. The traverse allows for constant velocity motion of the airfoil. The angle of attack can be altered from 1° to 8° in 1° increments. The velocity field is obtained by using time resolved planar particle image velocimetry which uses a 1W FN Series Dragon Laser, a Photron Fastcam Mini WX50 camera with a 100mm lens and polyamide seeding particles 20μm in diameter. Images were acquired at 750fps and were post processed using LaVision's DaVis 10.1 software. Images were preprocessed with a subtract sliding average filter to minimise noise. A multipass variable window size processing method was employed. The first four passes used a 64×64 pixel window with 1:1 square weighting and 50% overlap. The final pass used a 24×24 pixel window with 1:1 circular weighting and 50% overlap. Once the velocity field is obtained, spatial derivatives of velocity are obtained by using a fourth order central differencing scheme. The setup is shown in Figure 1

DESIGN SPACE

The three initial conditions of this experiment are the airfoil angle of attack (α), the distance through which the airfoil is surged, (Δx) and the speed at which it is surged ($U_{\text{surge}} = \Delta\dot{x}$). The upper limit of the surge distance was chosen as one chord length, so that wall effects introduced by the tank would not affect the wake. The lower limit of Δx was chosen such that the starting vortex and shear layer system had adequate time to develop before the field was contaminated by a stopping vortex formed at the end of airfoil motion. Huang *et. al* (2001) demonstrated in their study on vortex formation and evolution on the suction surface of an impulsively started NACA0012 wing that there are five distinct regimes of vortex evolution based on angle of attack and chord based Reynolds number. At angles of attack lower than 10°, a separation region was not observed on the suction side for all Reynolds

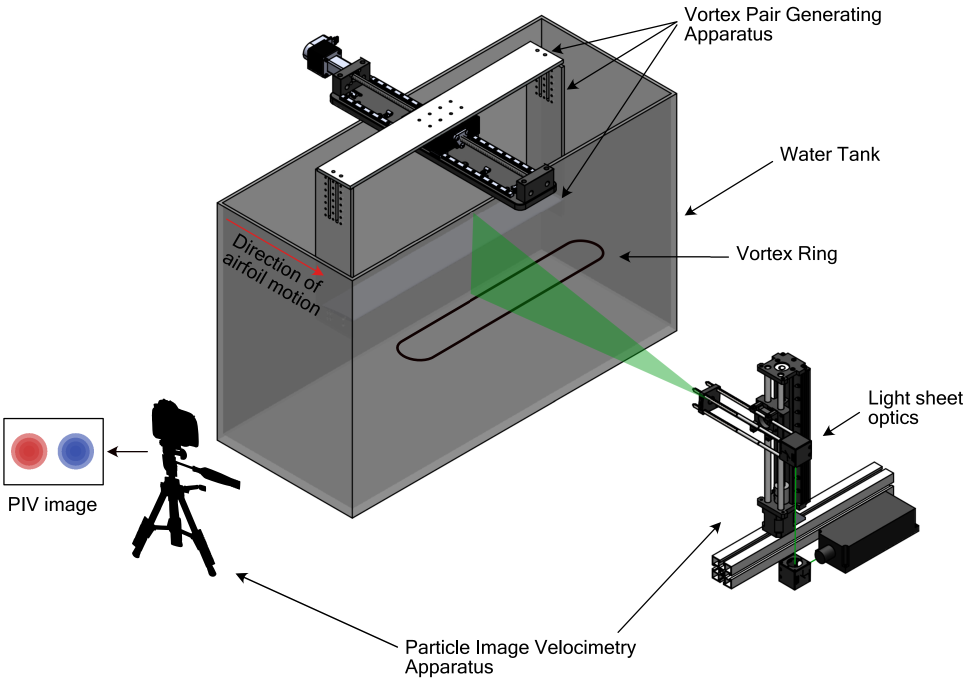

Figure 1. Vortex pair generating apparatus and PIV setup for the present experiment

numbers considered. For the present study, the highest angle of attack was chosen to be 7° to avoid flow separation. A lower limit of 3° was set, in part due to the weak vorticity that would be produced and challenges in obtaining accurate measurements. Finally, a range of surge speeds were tested and two distinct regimes of the wake were identified: one at surge speeds lower than a critical speed, U_{critical}, where the feeding shear layer remains intact and the other at surge speeds greater than U_{critical}, where the feeding shear layer breaks into smaller, Kelvin-Helmholtz type secondary vortices. The critical surge speed was found to be a function of the angle of attack: lower angles of attack resulted in higher values of U_{critical}.

TRAILING EDGE VELOCITY

The velocity field at the trailing edge was extracted whilst the airfoil was surging. For a case without secondary vortices, *i.e.,* for $U_{\text{critical}} < U_{\text{surge}}$, it was observed that both components of velocity were periodic, as shown in Figure 2. The contours for $u = 0$ and $v = 0$ are highlighted and show that the u component inflects along y at every time step. Furthermore, the v component is perfectly correlated with u- an increase in u results in the positive v component and a decrease results in a negative v component, thus showing that the peaks and crests of both components are correlated. Note that the first peak (and crest) is associated with the starting vortex.

Contours of u and v are extracted at the trailing edge for three different surge speeds at an angle of attack of 7°- $U_{\text{surge}} < U_{\text{critical}}$, $U_{\text{surge}} \to U_{\text{critical}}$ and $U_{\text{surge}} > U_{\text{critical}}$, as shown in Figure 3. Secondary vortices do not form in the first two cases and the third case shows four secondary vortices. To investigate the velocity field that results in secondary vortex formation, the shear layer was discretised as follows. A necessary condition for vortex formation is inflection in both components of velocity across the vortex centre. Since the airfoil surges from left to right, the vorticity associated with the starting vortex and trailing edge shear layer is in the clockwise direction. Thus, for a secondary vortex to form, the inflection in v must be from positive to negative across the vortex centre. Using the velocity field at the trailing edge shown in Figure 2, points across which both components of velocity inflect and the v component inflects from positive to negative are shown in Figure 4.

Once potential vortex centres were identified, the velocity field surrounding those points, containing one cycle of u and v were identified, shown by the dotted lines in Figure 4. Thus, the shear layer was discretised into potential vortex patches, which may or may not form a secondary vortex.

The objective of the following section is to describe the velocity fields within vortex patches.

VELOCITY FIELD

Let us consider a steady vortex, where the vortex centre is the origin, as shown in Figure 5. A cartesian coordinate system can be defined, such that u is the streamwise velocity along x and v is the cross stream vortex along y. Along y, the u component of velocity increases from zero, to a maxima, tends to zero at the vortex centre, inflects across the vortex centre, tends to a minima and once again, tends to zero. The v component of velocity similarly varies along x. At $y > 0$, a spatial average of the positive velocity, $\overline{U}_p$ can be computed and a spatial average of the negative velocity, $\overline{U}_n$, can similarly computed at $y < 0$. Similar spatial averages of v can be taken at $x < 0$ and $x > 0$ and are denoted as $\overline{V}_p$ and $\overline{V}_n$, respectively. A line joining $\overline{U}_p$ and $\overline{U}_n$ would form a 90° angle with the x and axis and a line joining $\overline{V}_p$ and $\overline{V}_n$ would form a 0° angle with the x axis. The steady u and v components would be orthogonal, even under a coordinate transformation.

Since we are studying vortex formation at short time scales, vortex patches do not exhibit the same, symmetric velocity distribution (and thus, orthogonality of the two velocity components) as steady vortices that are shown in Figure 5. The velocity distribution varies for different surge speeds at

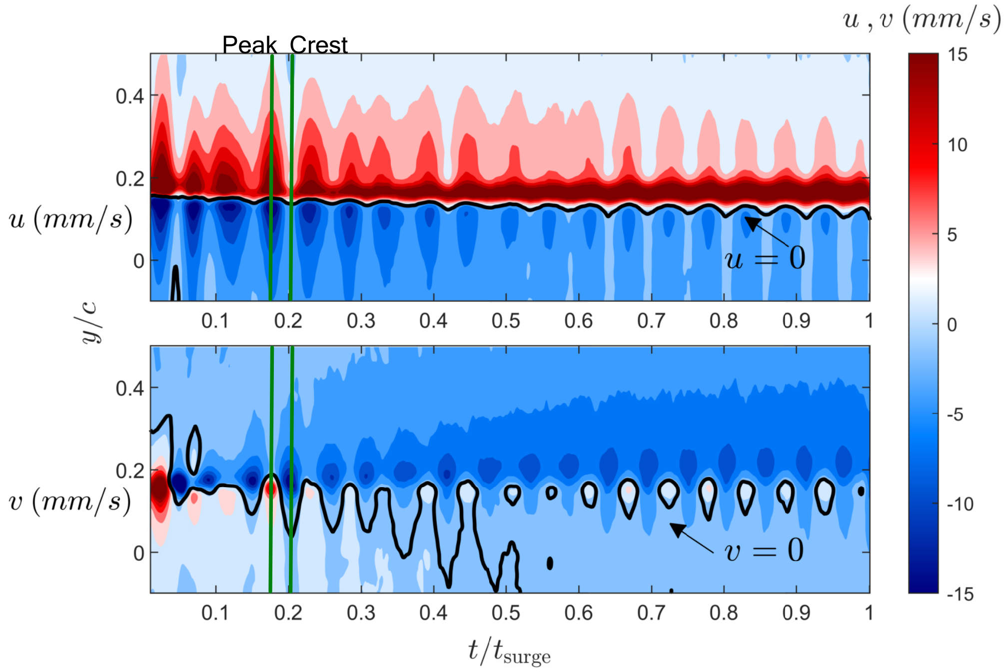

Figure 2. Velocities at the trailing edge for $U_{\text{surge}} < U_{\text{critical}}$, showing periodicity in both components of velocity. The contours of $u = 0$ and $v = 0$ are also highlighted.

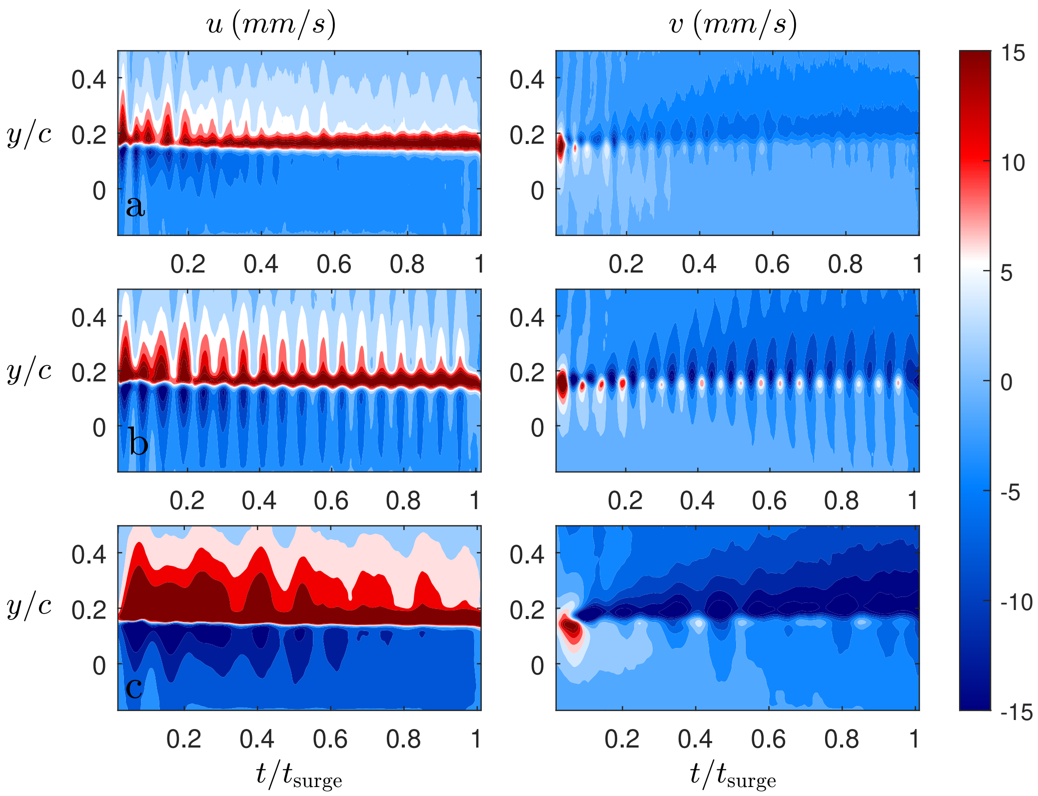

Figure 3. Contours of streamwise and cross streamwise velocities (u and v, respectively) for a) $U_{\text{surge}} < U_{\text{critical}}$, b) $U_{\text{surge}} \rightarrow U_{\text{critical}}$ and $U_{\text{surge}} > U_{\text{critical}}$

a given angle of attack. Consider the second vortex patch formed after the starting vortex, at an angle of attack of 7° for two surge speeds: $U_{\text{surge}} < U_{\text{critical}}$ and $U_{\text{surge}} > U_{\text{critical}}$, as shown in Figures 6 and 7, respectively.Both u and v velocities (in the cartesian coordinate system) show inflection within the vortex patch, across the vortex patch centre. Zero veloc-

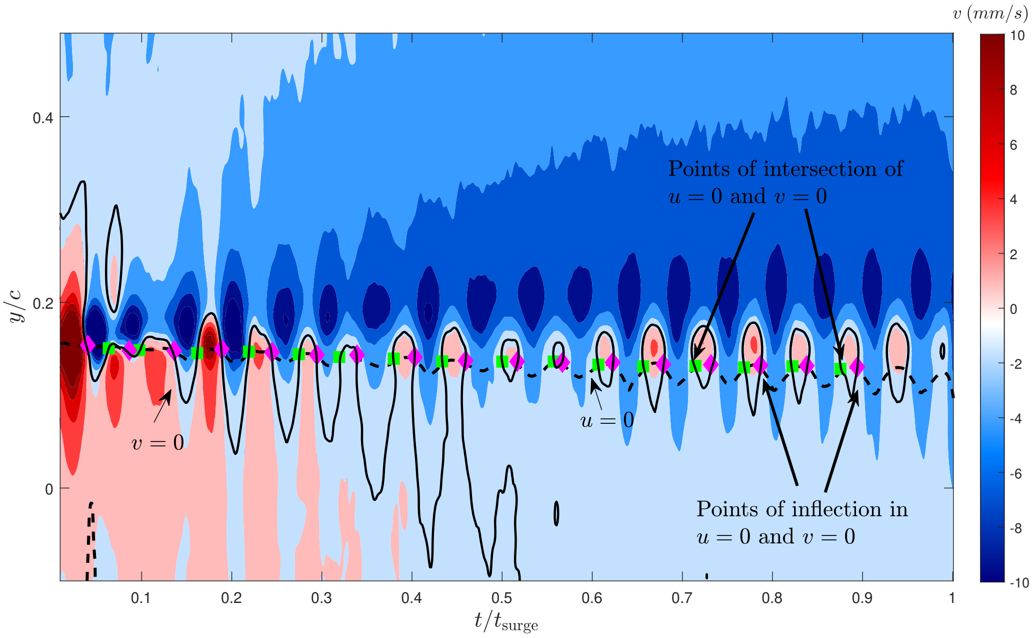

Figure 4. Contours of v in mm/s, superimposed with $u = 0$ in the dashed curve and $v = 0$ in the solid curve. Marked points are those where $u = 0$ and $v = 0$ intersect and v inflects from positive to negative. The dashed lines represent space enclosed by one cycle of u and v

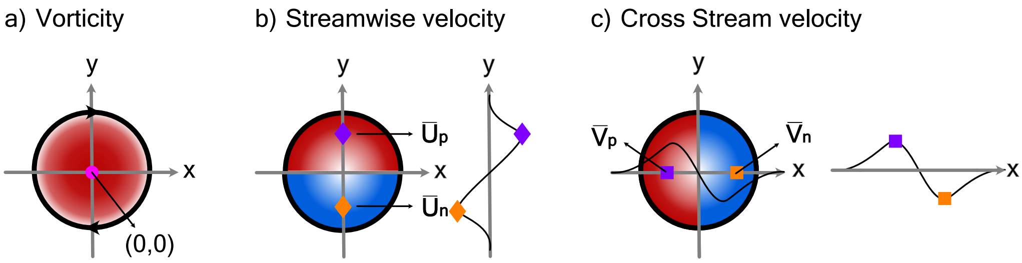

Figure 5. a) Vorticity, b) Streamwise velocity and c) Cross stream velocity distribution for a steady vortex. Spatial averages of positive and negative u, $\overline{U}_p$ and $\overline{U}_n$ are denoted. Spatial averages of positive and negative v, $\overline{V}_p$ and $\overline{V}_n$ are denoted.

ity contours are highlighted in the figures as well. An average of the positive and negative velocities can be taken within the vortex patch, as well as an averaged position where each averaged velocity acts. The velocity averages are an indication of the vortex strength, while the averaged positions are indicators of where the velocities act. We further define a line that joins the averaged velocities for each component. The angle that the line makes with the x axis can be used as a metric for determining how the velocity distribution changes over time. For the u component, an angle of 90° corresponds to that of a steady vortex and for the v component, an angle of 0° corresponds to a steady vortex. In Figure 6, we observe that the line joining the averaged u components maintains a 90° angle with the x axis. The line joining the averaged v components also remains closer to 90°, as compared to 0°. At a higher surge speed, beyond U_{critical}, shown in Figure 7, the line joining the averaged u components remains close to 90°, but that joining the v components is close to 0°, which would be the case for a steady vortex. To get an idea of how close the velocity distributions are to a steady case, we could look at the relative angle between the two lines (one for each component of velocity). Figure 8 show the relative angle between the lines joining the averaged u and v components. For the surge speed lower than U_{critical}, the angle between the two components is close to 0°, whereas for $U_{\text{surge}} > U_{\text{critical}}$, the angle between the two lines is closer to 90°, thus showing orthogonality between the two components, which is the case for steady vortices.

CONCLUSIONS AND FUTURE WORK

Experiments on impulsively started airfoils were performed at angle of attack smaller than stall. Two flow regimes were identified for a given angle of attack- one where the shear layer remains intact and another where the shear layer breaks into smaller, Kelvin-Helmholtz type vortices. The velocity at the trailing edge was extracted for each time step and it was found that both components of velocity show periodicity for both regimes. The shear layer was further discretised into vortex patches based on the periodicty of the velocity field, with each vortex patch isolated as one cycle of u (and v). The velocity fields of the discretised shear layers were analysed and a salient difference between the velocity fields with and without secondary vortices was the rotation of the v component of velocity, resulting in orthogonality between the two velocity components at surge speeds greater than U_{critical}.

Velocity gradients within vortex patches can be used to compute the strains and rotation of each vortex patch. The gradients can further be used to devise a critical parameter that determines secondary vortex formation in shear layers. Since secondary vortices are typical features of impulsive starting

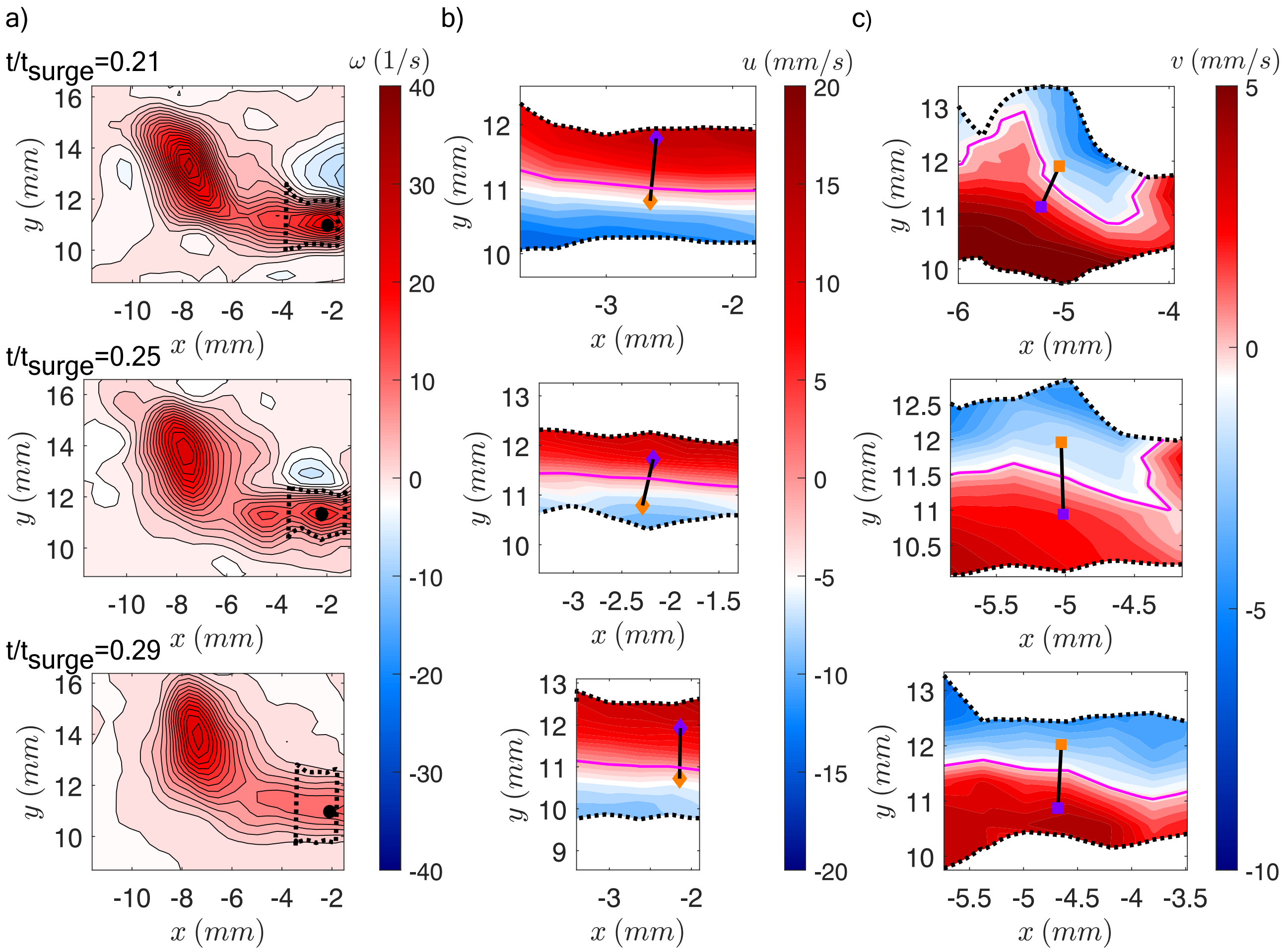

Figure 6. a) Vorticity, b) Streamwise and c) Cross streamwise velocity contours for the second vortex patch at $U_{\text{surge}} < U_{\text{critical}}$ at three different times (non-dimensionalised by the surge time, t_{surge}).

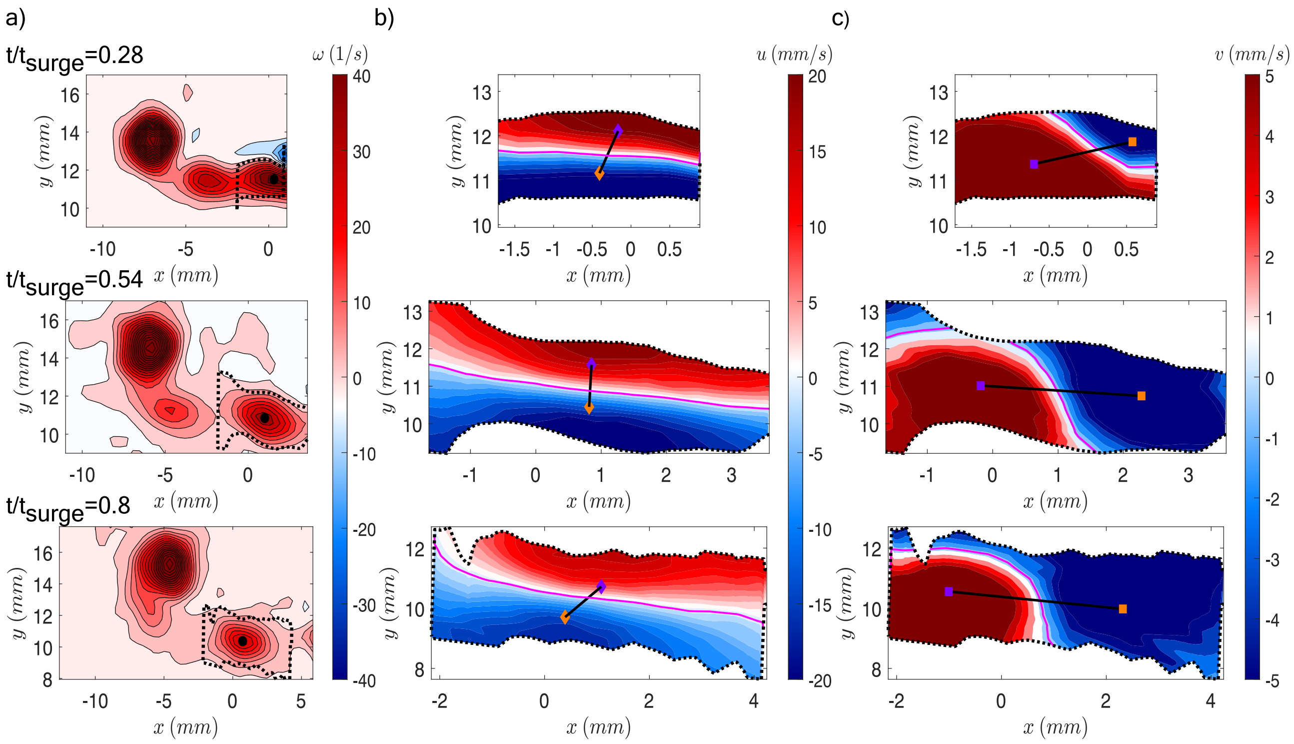

Figure 7. a) Vorticity, b) Streamwise and c) Cross streamwise velocity contours for the second vortex patch at $U_{\text{surge}} > U_{\text{critical}}$ at three different times (non-dimensionalised by the surge time, t_{surge}).

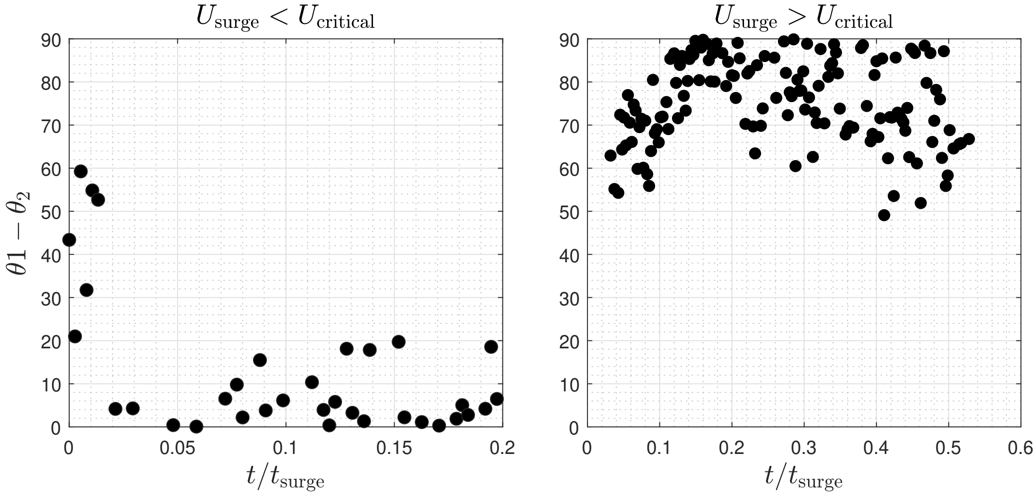

Figure 8. Relative angles between the line joining spatial average of u (θ_1) and v (θ_2) for $U_{\mathrm{surge}} < U_{\mathrm{critical}}$ and $U_{\mathrm{surge}} > U_{\mathrm{critical}}$

flows, such a critical parameter would deepen our understanding of starting flows.

REFERENCES

DeVoria, Adam C & Ringuette, Matthew J 2012 Vortex formation and saturation for low-aspect-ratio rotating flat-plate fins. *Experiments in fluids* **52**, 441–462.

Fernando, John N & Rival, David E 2016 On vortex evolution in the wake of axisymmetric and non-axisymmetric low-aspect-ratio accelerating plates. *Physics of Fluids* **28** (1).

Ford, CW Pitt & Babinsky, Holger 2013 Lift and the leading-edge vortex. *Journal of Fluid Mechanics* **720**, 280–313.

Francescangeli, Diego & Mulleners, Karen 2023 Strength and timing of primary and secondary vortices generated by a rotating plate. *Experiments in Fluids* **64** (7), 128.

Huang, Rong F. & Lin, Chih L. 1995 Vortex shedding and shear-layer instability of wing at low-reynolds numbers. *AIAA Journal* **33** (8), 1398–1403.